



---

Year: 2015

---

## PAX6 expression and retinal cell death in a transgenic mouse model for acute angle-closure glaucoma

Stanescu-Segall, Dinu ; Birke, Kerstin ; Wenzel, Andreas ; Grimm, Christian ; Orgul, Sorguel ; Fischer, Jan A ; Born, Walter ; Hafezi, Farhad

**Abstract:** **PURPOSE:** PAX6 is a highly conserved protein essential for the control of eye development both in invertebrates and vertebrates. PAX6 expression persists in the adult inner retina, but little is known about its functions after completion of retinal differentiation. Therefore, we investigated PAX6 expression in wild-type and calcitonin receptor-like receptor transgenic (CLR) mice with angle-closure glaucoma. **METHODS:** Intraocular pressure was measured by indentation tonometry in anesthetized mice. Eyes of mice of both genotypes were enucleated at various ages and retinas were processed for morphological analysis and PAX6 immunostaining. The content of PAX6 in retinal extracts was estimated by Western blot analysis. Retinal expression of glaucoma-related genes was analyzed by reverse transcription-polymerase chain reaction. **RESULTS:** Control mice showed normal retinal morphology between p22 and p428 with steady PAX6 expression in the ganglion cell layer (GCL) and the inner nuclear layer (INL). CLR mice examined between p22 and p82 exhibited increased intraocular pressure and a progressive decrease in cell number including PAX6-expressing cells in the GCL. The INL was not affected up to postnatal day 42. Later, a significant increase in PAX6-expressing cells concomitant with an overall loss of cells was observed in the INL of CLR as compared with control mice. Retinal up-regulation of glaucoma-related genes was furthermore observed. **CONCLUSIONS:** Distinctive changes of PAX6 expression in the inner retina of CLR mice suggest a role in regulatory mechanisms involved in glaucoma-related retinal cell death. The selective increase of PAX6 expression in the degenerating INL of CLR mice may represent an attempt to preserve retinal cytoarchitecture.

DOI: <https://doi.org/10.1097/IJG.0b013e318207069b>

Posted at the Zurich Open Repository and Archive, University of Zurich

ZORA URL: <https://doi.org/10.5167/uzh-111477>

Journal Article

Published Version

Originally published at:

Stanescu-Segall, Dinu; Birke, Kerstin; Wenzel, Andreas; Grimm, Christian; Orgul, Sorguel; Fischer, Jan A; Born, Walter; Hafezi, Farhad (2015). PAX6 expression and retinal cell death in a transgenic mouse model for acute angle-closure glaucoma. *Journal of Glaucoma*, 24(6):426-432.

DOI: <https://doi.org/10.1097/IJG.0b013e318207069b>

# PAX6 Expression and Retinal Cell Death in a Transgenic Mouse Model for Acute Angle-Closure Glaucoma

Dinu Stanescu-Segall, MD,\* Kerstin Birke, PhD,† Andreas Wenzel, PhD,‡ Christian Grimm, PhD,‡  
Sorguel Orgul, MD, PhD,§ Jan A. Fischer, PhD,† Walter Born, PhD,† and Farhad Hafezi, MD, PhD||

**Purpose:** PAX6 is a highly conserved protein essential for the control of eye development both in invertebrates and vertebrates. PAX6 expression persists in the adult inner retina, but little is known about its functions after completion of retinal differentiation. Therefore, we investigated PAX6 expression in wild-type and calcitonin receptor-like receptor transgenic (CLR<sup>SM $\alpha$ A</sup>) mice with angle-closure glaucoma.

**Methods:** Intraocular pressure was measured by indentation tonometry in anesthetized mice. Eyes of mice of both genotypes were enucleated at various ages and retinas were processed for morphological analysis and PAX6 immunostaining. The content of PAX6 in retinal extracts was estimated by Western blot analysis. Retinal expression of glaucoma-related genes was analyzed by reverse transcription-polymerase chain reaction.

**Results:** Control mice showed normal retinal morphology between p22 and p428 with steady PAX6 expression in the ganglion cell layer (GCL) and the inner nuclear layer (INL). CLR<sup>SM $\alpha$ A</sup> mice examined between p22 and p82 exhibited increased intraocular pressure and a progressive decrease in cell number including PAX6-expressing cells in the GCL. The INL was not affected up to postnatal day 42. Later, a significant increase in PAX6-expressing cells concomitant with an overall loss of cells was observed in the INL of CLR<sup>SM $\alpha$ A</sup> as compared with control mice. Retinal up-regulation of glaucoma-related genes was furthermore observed.

**Conclusions:** Distinctive changes of PAX6 expression in the inner retina of CLR<sup>SM $\alpha$ A</sup> mice suggest a role in regulatory mechanisms involved in glaucoma-related retinal cell death. The selective increase of PAX6 expression in the degenerating INL of CLR<sup>SM $\alpha$ A</sup> mice may represent an attempt to preserve retinal cytoarchitecture.

**Key Words:** PAX6, human, angle-closure, glaucoma, retinal degeneration, ganglion cells

(*J Glaucoma* 2015;00:000–000)

Received for publication February 22, 2010; accepted November 14, 2010.

From the \*Department of Ophthalmology, Charing Cross Hospital, Imperial College London, London, UK; †Research Laboratory, Orthopaedic University Hospital Balgrist; ‡Department of Ophthalmology, Laboratory for Retinal Cell Biology, University Hospital Zurich; §IROC, Institute for Refractive and Ophthalmic Surgery, Zurich; and ||University Eye Clinic Basel, Basel, Switzerland.

Disclosure: Supported by the Swiss National Science Foundation (SNF), the University of Zurich, and the Schweizerischer Verein Balgrist. The authors had no financial relationship with these organizations and have full control of all primary data.

K.B. and D.S.-S. have equally contributed to the paper. Reprints: Dinu Stanescu-Segall, MD, Department of Ophthalmology, Charing Cross Hospital, Imperial College London, London, United Kingdom (e-mail: dinustanescu@gmail.com).

Copyright © 2015 Wolters Kluwer Health, Inc. All rights reserved. DOI:10.1097/IJG.0b013e318207069b

PAX6, a member of the paired box family of transcription factors, is an essential control gene for eye morphogenesis both in invertebrates and vertebrates.<sup>1–3</sup> Its importance for eye development was demonstrated in several species. The human and murine (small eye) PAX6 protein are identical in their amino acid sequence, and the *Drosophila* homolog (Eyeless) shows over 90% identity over the paired and the homeodomain.<sup>4</sup> Moreover, gain-of-function studies demonstrated that targeted expression of *Drosophila* and PAX6 induces ectopic eyes in *Drosophila*.<sup>5</sup>

Mutations in PAX6 lead to a variety of eye abnormalities including hereditary foveal hypoplasia, optic nerve malformation, and aniridia in mice<sup>6–9</sup> and humans.<sup>10–18</sup>

PAX6 has been studied extensively in eye and retinal development. Normal development of the inner retina is directly influenced by a well-elaborated spatial and temporal pattern of PAX6 expression.<sup>1,6–9,19–21</sup> However, little is known about PAX6 expression and function in the adult mammalian retina. De Melo et al<sup>22</sup> showed that several homeobox genes including *Pax6* are expressed in the young adult mouse retina and we recently reported continuous expression of PAX6 in the young, adult, and old normal human retina.<sup>23</sup>

To investigate the role of PAX6 expression in the adult eye and to assess whether PAX6 is involved in degenerative processes of the retina, we studied PAX6 expression in wild type and in calcitonin receptor-like receptor transgenic (CLR<sup>SM $\alpha$ A</sup>) mice with acute angle-closure glaucoma (ACG).<sup>24</sup>

## MATERIALS AND METHODS

All animal experiments conformed to the guidelines of the Veterinary Authorities of the Kanton of Zurich and to the statement of the Association for Research in Vision and Ophthalmology for the use of Animals in Ophthalmic and Vision Research.

### Animals

CLR<sup>SM $\alpha$ A</sup> mice were generated and genotyped together with wild-type littermates as reported.<sup>24</sup> Three CLR<sup>SM $\alpha$ A</sup> mice and 3 control littermates were analyzed at indicated ages in individual experiments. Animals were sacrificed by cervical dislocation and experiments were performed in triplicates.

### Measurement of Intraocular Pressure

Intraocular pressure (IOP) was measured by indentation tonometry in anesthetized mice as described previously.<sup>24</sup> An average of 6 readings was considered as a single result; presented values are the average of 10 eyes per genotype at each time point (same mice at different ages).

## Retinal Morphology

Eyes were prepared as described previously.<sup>25</sup> Briefly, mice were sacrificed and enucleated eyes were fixed with 2.5% glutaraldehyde in 0.1 M cacodylate buffer, pH 7.3, at 4°C overnight. The eyes were then washed in cacodylate buffer, incubated in osmium tetroxide for 1 hour, dehydrated in ascending ethanol series, and embedded in Epon 812 (Sigma-Aldrich, St. Louis, MO). Central retinal sections (0.5 µm; temporal-nasal) were stained with toluidine blue (Sigma-Aldrich, St. Louis, MO) and analyzed by light microscopy.

## Retinal Morphometry

CLR<sup>SMaA</sup> and control mice were sacrificed and the eyes were enucleated and fixed by immersion in 4% paraformaldehyde in phosphate-buffered saline overnight. The eyes were then dehydrated and embedded in paraffin according to standard protocols. Paraffin sections (5 µm) were deparaffinized in xylene, hydrated in descending ethanol series, and stained with toluidine blue. The sections were then washed with water, dehydrated in ethanol, and mounted with DPX (Sigma-Aldrich, St. Louis, MO). Morphometry in the ganglion cell layer (GCL) and inner nuclear layer (INL) of CLR<sup>SMaA</sup> and control littermates was performed by counting all cells in the respective layers on 5 µm central sagittal sections under the microscope at 40-fold magnification with the ImageJ software (<http://rsb.info.nih.gov/ij/>; version 1.36a). Data were collected from 3 sections per eye of 3 CLR<sup>SMaA</sup> and 3 age-matched control littermates.

## Retinal Immunohistochemistry

Central sagittal sections were boiled at 95°C for 20 minutes in citrate buffer and incubated in blocking reagent (Vector Laboratories, Burlingame, CA) at room temperature for 60 minutes. The sections were then incubated at 4°C overnight with polyclonal rabbit antibodies to PAX6 (1:300) (Chemicon, Temecula, CA). PAX6 immunostaining was visualized with secondary biotinylated antibodies to rabbit IgG (1:200) (Vector Laboratories, Burlingame, CA) and Cy3-labeled streptavidin (1:200) (Sigma-Aldrich, St. Louis, MO). Fluorescence was detected with a DX20 CCD camera (Kappa, Gleichen, Germany) connected to a 0.45 × projection lens of an Eclipse E600 Nikon microscope equipped with a Plan Fluor 20 × /0.5 DLL objective and a G-2A (Cy3) filter block.

## Western Blot Analysis

Retinas were rapidly dissected through a slit in the cornea using the Winkler technique.<sup>26</sup> The tissue was sonicated in 100 mM Tris/HCl, pH 7.5, containing complete protease inhibitor cocktail tablets (Roche Diagnostics, Rotkreuz, Switzerland). Retinal extracts were cleared by centrifugation and proteins were separated by sodium dodecyl sulfate-polyacrylamide gel electrophoresis (12%) and then electrotransferred to nitrocellulose Hybond enhanced chemiluminescent membranes (GE Healthcare Europe GmbH, Otelfingen, Switzerland) in a Trans-Blot SD semi-dry transfer cell (Bio-Rad Laboratories, Hercules, CA). The membranes were blocked with 5% low fat milk. PAX6 was detected with corresponding polyclonal antibodies (1:5000) (Chemicon, Temecula, CA) and alkaline phosphatase-conjugated secondary antibodies (1:15,000) (Sigma-Aldrich, St. Louis, MO). PAX6 was normalized to actin as a protein loading control. Actin was detected with

mouse monoclonal antibodies to actin (1:5000) (Sigma, Buchs, Switzerland) and alkaline phosphatase-conjugated secondary antibodies (1:15,000) (Sigma-Aldrich, St. Louis, MO). Alkaline phosphatase activity was visualized with the Bio-Rad detection kit (Bio-Rad Laboratories, Hercules, CA) and a VersaDoc Imaging System (Bio-Rad Laboratories, Hercules, CA).

## Reverse Transcription and Semi-quantitative Polymerase Chain Reaction

Retinas were prepared from CLR<sup>SMzA</sup> mice and control littermates as described above and frozen in liquid nitrogen. Total RNA was isolated with the RNeasy kit (QIAGEN, Hilden, Germany) and cDNA was generated with Moloney Murine leukemia virus reverse transcriptase (Promega, Madison, WI). Polymerase chain reaction was carried out with primers specific for glial fibrillary acidic protein (GFAP) (forward: 5'-CCACAACTGGCTGATGTCTAC-3', reverse: 5'-TTCTCTCCAAATCCACACGAGC-3'); tissue inhibitors of metalloproteinase-1 (TIMP-1) (forward: 5'-AGAAATCAACGAGACCACCT-3', reverse: 5'-GGGCTCAGAGTACGCCA-3'); interleukin-1b (IL-1b) (forward: 5'-GCAGGCAGTATCACTCATTG-3', reverse: 5'-CGTTGCTTGGTCTCCTTGT-3'); Endothelin-2 (forward: 5'-TTGTGAGTGCTCTACTGCG-3', reverse: 5'-GGTGTATCTCTCCATCT-3'); X-linked inhibitor of apoptosis (XIAP) (forward: 5'-GGATCCTCTGATGCTGTGAGTTCTGATAGGAATTTCCC-3', reverse: 5'-GACTCGAGCTAAGTAGTTCTTACCAGACACTCCTCAAG-3'); Bcl-X<sub>L</sub> (forward: 5'-GACTTTCTCTCTACAAGC-3', reverse: 5'-CGAAAGAGTTCATTCCTACTAC-3'); Bcl-2 (forward: 5'-TTGTGGCCTTCTTTGAGTTCG-3', reverse: 5'-ATTTCTACTGCTTTAGTGAACC-3'); and glyceraldehyde 3-phosphate dehydrogenase (forward: 5'-GGGTGGAGCCAAACGGGTC-3', reverse: 5'-GGAGTTGC-TGTTGAAGTCGCA-3') with Roche LightCycler reagents. Polymerase chain reaction products were separated and quantified on agarose gels by densitometry.

## Statistical Analysis

Results are presented as the mean ± standard error of the mean. Differences between mean values were analyzed by analysis of variance using the Prism 3.0 software (GraphPad Software Inc, San Diego, CA). *P* < 0.05 was considered statistically significant.

## RESULTS

### PAX6 is Expressed in the Inner Retina Throughout the Lifespan of Wild-type Mice

Retinal morphology and PAX6 expression were examined in wild-type mice at postnatal days (p) 5, 9, 15, 20, 24, 29, 243, and 428. Retinal morphology was normal in all mice analyzed (Fig. 1A, representative retinal section at p29). PAX6 expression was confined mainly to nuclei of cells in the inner part of the INL and, to a lesser extent, to the GCL at all time points tested (Fig. 1B, representative section at p29). Western blot analysis showed continuous expression of PAX6 from p5 to p428 with a minimal decrease between p5 and p20 (Fig. 1C).

### Retinal Damage in CLR<sup>SMzA</sup> Mice With Increased Ocular Pressure

CLR<sup>SMzA</sup> mice presented normal IOP at the end of ocular development on p20 (Fig. 2A). Subsequently, the IOP increased up to p62 to over 2-time higher levels than in

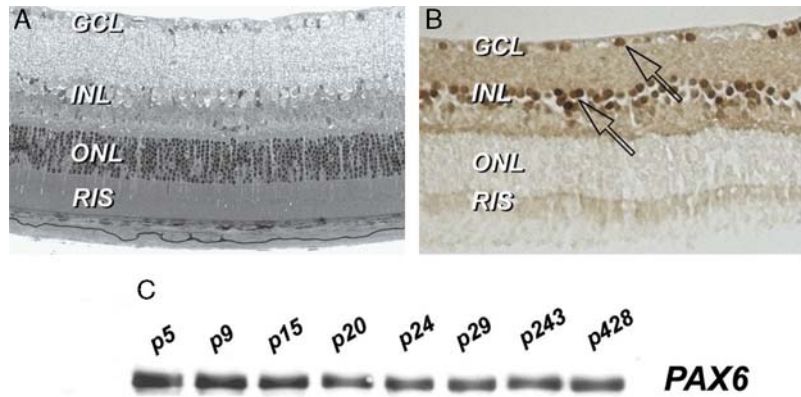


**FIGURE 1.** PAX6 expression in the retina of wild-type mice. Morphological analysis at p29 shows normal cytoarchitecture of the outer and inner retina (Epon embedding, methylene blue staining) (A). Immunohistochemical PAX6 staining at p29 revealed PAX6 expression confined to the nuclei of the inner nuclear layer (INL) and the ganglion cell layer (GCL) (arrows) (B). The rod inner segments (RIS) and the outer nuclear layer (ONL) are also shown. Western blot analysis of PAX6 expression in the retina of mice at indicated ages (C). Equal amounts of protein were loaded. p29 indicates postnatal day 29.

control mice. Consequently, the number of apoptotic terminal deoxynucleotidyl transferase dUTP nick end labeling-stained cells in the GCL of *CLR<sup>SMzA</sup>* mice was higher than in control animals (not shown). Moreover, the

expression of genes indicating gliosis or apoptosis of the glaucomatous retina was also altered in *CLR<sup>SMzA</sup>* mice (Table 1). On p32, the gliosis-related GFAP and endothelin-2 gene-derived transcripts were found up-regulated in

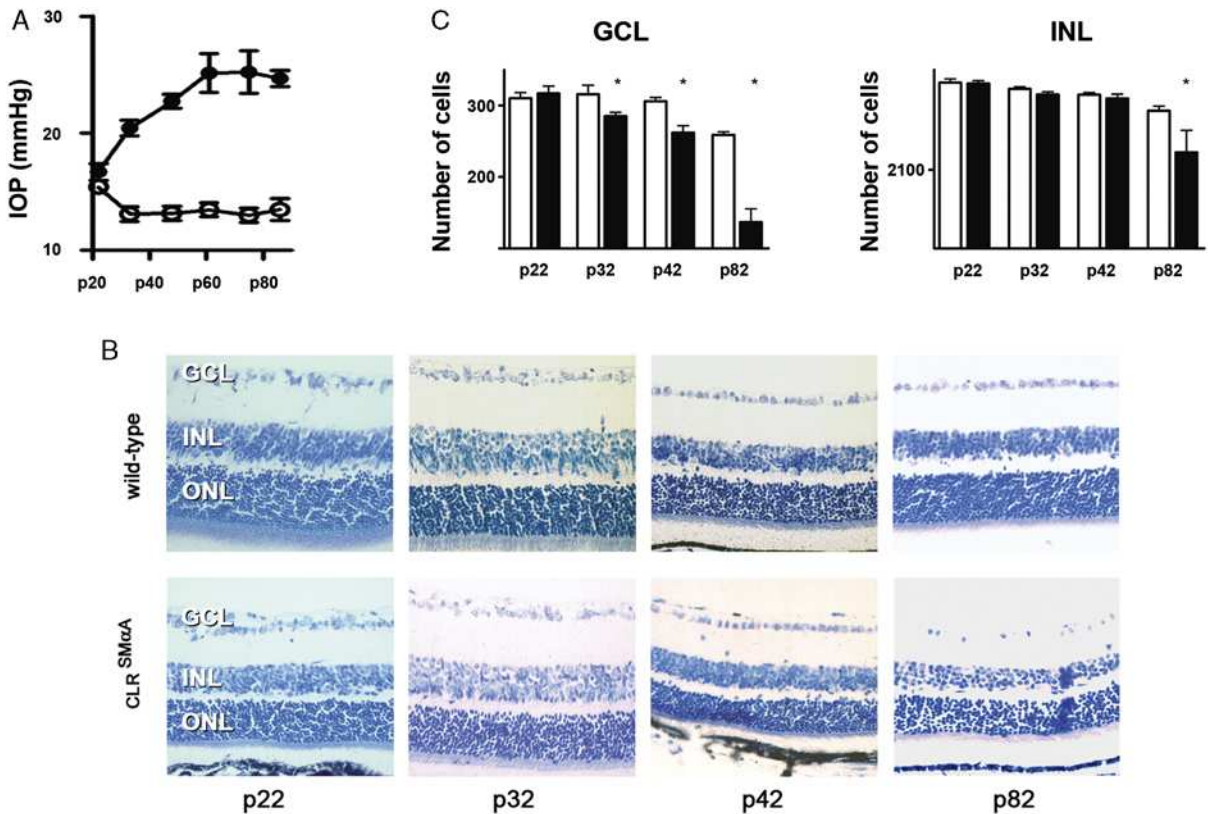


**FIGURE 2.** Increase in IOP over time in *CLR<sup>SMzA</sup>* mice (●) as compared with control littermates (○) (A). Data are mean (±SEM) of IOP measurements in at least 10 *CLR<sup>SMzA</sup>* and 10 control mice per time point. Morphology of the ganglion cell layer (GCL), the inner nuclear layer (INL), and the outer nuclear layer (ONL) in representative 5-μm toluidine blue-stained central sagittal sections of the retina of *CLR<sup>SMzA</sup>* and control (wild-type) mice at indicated ages (B). Morphometric analysis of the GCL and the INL in control (open bars) and *CLR<sup>SMzA</sup>* mice (closed bars) at indicated ages (C). Data are mean±SEM of 3 sections per eye from 3 controls and 3 *CLR<sup>SMzA</sup>* mice per time point. IOP indicates intraocular pressure; SEM, standard error of mean.

**TABLE 1.** Relative Expression Levels of Apoptosis-related Gene Transcripts Determined by Reverse Transcription-polymerase Chain Reaction in Retinal RNA Extracts of CLR<sup>SMαA</sup> Compared With Control Mice

mRNA	p32	p82
GFAP	2.95	0.78
TIMP-1	16.85	24.53
IL-1b	1.69	1.47
Endothelin-2	11.45	17.98
XIAP	0.96	0.29
Bcl-X <sub>L</sub>	1.20	0.69
Bcl-2	1.02	0.42

Bcl-2 indicates B-cell leukemia/lymphoma-2; Bcl-X<sub>L</sub>, B-cell leukemia/lymphoma extra long; GFAP, glial fibrillary acidic protein; IL-1b, interleukin-1b; TIMP-1, tissue inhibitor of metalloproteinase-1; XIAP, X-linked inhibitor of apoptosis.

CLR<sup>SMαA</sup> as compared with control animals. Endothelin-2, unlike GFAP transcripts, remained up-regulated on p82. The TIMP-1 encoding transcripts, similar to those for endothelin-2, were up-regulated on p32 and p82. Consistent with the ongoing apoptosis in the retina of CLR<sup>SMαA</sup> mice, IL-1b transcripts were up-regulated on p32 and p82, and XIAP transcripts and those encoding the anti-apoptotic proteins Bcl-X<sub>L</sub> and Bcl-2 were lower than in control mice on p82.

Retinal morphology was normal in CLR<sup>SMαA</sup> mice at p22 (Figs. 2B, C). Subsequently, the number of cells in the GCL of CLR<sup>SMαA</sup> mice decreased more rapidly than in control littermates. The INL, on the other hand, showed similar and unchanged morphological and morphometric features in control and CLR<sup>SMαA</sup> mice up to p42. At p82,

however, the cell number in the INL was significantly lower ( $P < 0.05$ ) in CLR<sup>SMαA</sup> than in control mice.

**PAX6 Expression in the Retina of CLR<sup>SMαA</sup> Mice**

PAX6 expression in the retina of CLR<sup>SMαA</sup> mice and control littermates was confined to the nuclei of the INL and GCL (Fig. 3A). In CLR<sup>SMαA</sup> mice, unlike in control littermates, the number of PAX6-expressing cells in the GCL decreased in parallel to the total number of cells between p22 and p82 (Fig. 2C, Fig. 3B). In the INL, on the other hand, the number of PAX6-expressing cells was indistinguishable in CLR<sup>SMαA</sup> and control mice up to p42, but, interestingly, on p82 the number of PAX6-expressing cells was significantly ( $P < 0.05$ ) higher in CLR<sup>SMαA</sup> than in control mice (Fig. 3). These morphometric and immunohistochemical results were consistent with transiently decreased levels of PAX6 on p42, p52, and p62 and subsequently increased levels on p72, reaching a peak at p82 and being sustained at higher levels until p102 in total retinal extracts of CLR<sup>SMαA</sup> as compared with control mice, recognized on Western blots (Fig. 4).

**DISCUSSION**

PAX6 is a transcription factor influencing eye morphogenesis in invertebrates and vertebrates.<sup>2,3</sup> Besides the striking amino acid sequence similarities of PAX6 in different species, conserved regulation of expression seems to be vital for ocular integrity.<sup>27</sup> Although PAX6 was extensively studied during eye organogenesis in various species, little is known about PAX6 expression and function in adult eye tissues. PAX6 expression in the GCL and INL of the inner retina was observed in humans,<sup>23</sup> chicken,<sup>28</sup> and mouse<sup>29</sup> and Zhang et al<sup>30</sup> detected PAX6 expression in the adult lens epithelium.

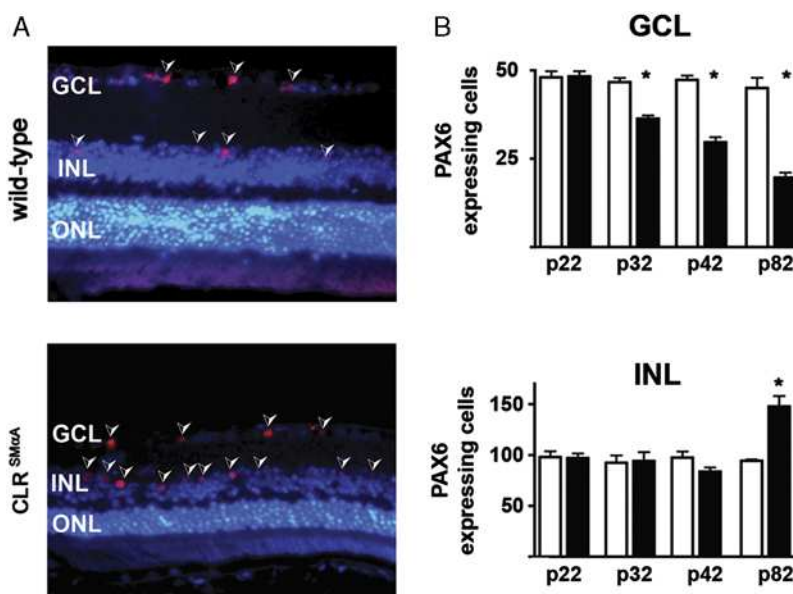


**FIGURE 3.** PAX6 expression in the ganglion cell layer (GCL) and the inner nuclear layer (INL) in control (wild-type) and CLR<sup>SMαA</sup> mice (A). Immunofluorescent staining of PAX6 (red, arrowheads) and 4',6'-diamidino-2-phenylindole staining of cell nuclei (blue) in the GCL and the INL of central retinal sections also including the outer nuclear layer (ONL) on p82. B, Morphometric analysis of PAX6 expression over time in the GCL and the INL from control (open bars) and CLR<sup>SMαA</sup> (closed bars) mice. Data are mean±SEM of 3 sections per eye from 3 control and 3 CLR<sup>SMαA</sup> mice per time point. \* $P < 0.05$  compared with control mice of the same age. p82 indicates postnatal day 82; SEM, standard error of mean.

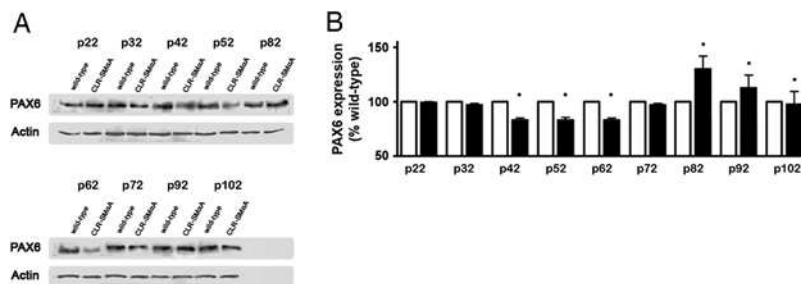


**FIGURE 4.** PAX6 expression over time was examined by Western blot analysis in retinal extracts of control (wild-type) and CLR<sup>SMzA</sup> mice. PAX6 and actin were visualized by enhanced chemiluminescence with corresponding antibodies. Representative for 3 independent experiments (A). Relative changes of PAX6 expression normalized to actin in the retina of CLR<sup>SMzA</sup> compared with control mice (B). The values obtained for the extracts of control mice at individual time points were set to 100%. Data are the mean ± SEM of 3 independent experiments. \**P* < 0.05 compared with control mice of the same age. Open bars refer to expression of control mice and closed bars refer to CLR<sup>SMzA</sup> mice. SEM indicates standard error of mean.

To further elucidate the potential roles of PAX6 in the inner retina of an adult eye, we investigated its expression in wild-type and CLR<sup>SMzA</sup> mice, a mouse model of acute ACG. ACG is very much underestimated and suspected to affect half of all glaucoma patient worldwide and accounts for 91% of bilateral glaucoma blindness in China.<sup>31</sup> ACG pathophysiology is largely unknown and CLR<sup>SMzA</sup> mouse model appears as a reliable mouse model for this disease. It offers the advantage to mimic human condition with transient IOP peaks between 1 and 3 months.<sup>24</sup> It obviates repetitive manipulations on the eyes of the mouse and costly equipment such as lasers needed for laser-induced increased IOP models.<sup>32–34</sup> It is also one of the few genetic rodent model that is amendable to experimental manipulation because of its shorter course of glaucomatous pathology.

These mice develop ACG after completion of retinal development<sup>24</sup> and, as shown here, suffer from progressive retinal ganglion cell loss.

The retina of CLR<sup>SMzA</sup> mice expressed elevated levels of GFAP, TIMP-1, IL-1b, and endothelin-2, which were also found to be up-regulated in glaucoma in previous studies. Increased GFAP is commonly observed in degenerative retinal diseases,<sup>35,36</sup> whereas TIMP-1–encoding mRNA is elevated in microglia of glaucoma patients.<sup>37</sup> Activation of proinflammatory IL-1b might be involved in the etiology of glaucoma<sup>35,38,39</sup> and increased endothelin-2 expression occurs in human glaucoma during glial activation.<sup>40</sup> Late down-regulation of the caspase inhibitor XIAP and of Bcl-X<sub>L</sub> and Bcl-2 was observed in CLR<sup>SMzA</sup> mice on p82, similar to observations in degenerating retinas.<sup>41–43</sup> As transgenic expression of XIAP was shown to increase survival of cells in the inner retina in mouse models of ischemia,<sup>44</sup> it seems likely that the reduced expression of this inhibitor of apoptosis contributes to the retinal pathology and the observed loss of neuronal cells.

Our results also show a decreased PAX6 expression in the GCL of CLR<sup>SMzA</sup> mice during the initial phase of ganglion cell degeneration. At p82, however, cells of the INL in CLR<sup>SMzA</sup> mice displayed a marked increase in PAX6 protein levels. At this time point, the GCL has lost about 75% of its cells (Fig. 2) and thus synaptic connectivity between bipolar, amacrine, and ganglion cells was severely disrupted. We found similar results in total protein extracts of CLR<sup>SMzA</sup> mice. Western blots of PAX6 showed an increase of its expression at p72, reaching a peak at p82, with a progressive decline from p92 until normal levels at p102.

In DBA/2J mouse, peak of retina ganglion cell (RGC) apoptosis varies between 6 and 11 months according to Schuettauf et al and Libby et al.<sup>45,46</sup> We speculate that in this mouse, PAX6 expression would have increased after the peak of GCL apoptosis. Although the length of time needed to obtain these results in DBA/2J was too long to be able to verify our hypothesis.

In laser-induced ocular hypertension mouse model of glaucoma, IOP is less elevated than in CLR<sup>SMzA</sup> mice and induce a moderate RGC reduction of 15% to 17% and 22% to 27% after 2 and 4 weeks, respectively after laser photocoagulation of the episcleral and limbal veins.<sup>32,33</sup> We believe that in this mice, a slight elevation of PAX6 expression would have occurred after 4 weeks but probably less pronounced than in our model because the apoptosis peak was less marked. Unfortunately, the cost of laser equipment precludes us from corroborating these data. We were less interested in studying PAX6 expression in RGC death after mechanical injury of the optic nerve,<sup>47</sup> intraocular injection of excitotoxic agents,<sup>48,49</sup> or by the induction of ischemia followed by reperfusion<sup>50</sup> because the pathophysiology in those systems does not directly follow that of human glaucoma.

It has been shown in models of photoreceptor degeneration that cells especially of the INL react to loss of neurons by the induction of a program leading to retinal remodeling (for review see Ref. 51). During the initial phase of photoreceptor loss, bipolar and horizontal cells are deafferented and retract most of their dendrites, and Muller cells increase the production of intermediate filaments. Although remodeling processes in models of glaucoma have not been studied in detail, Marc and coworkers<sup>51</sup> showed that the space left by degenerated ganglion cells in retinitis pigmentosa retinas was filled at least in part by Muller cell end feet. Interestingly, Jones and coworkers have demonstrated that PAX6 expression is increased in cells of the INL during retinal degeneration in the rd1 mouse,<sup>29</sup> concomitantly with the early phase of remodeling processes. As PAX6 regulates eye development including retinal morphogenesis,<sup>52</sup> it is conceivable that increased PAX6 production during degeneration is required for surviving cells to adapt to the altered conditions by changing their cytoarchitecture. This is supported by observations that expression levels of PAX6 can severely influence the overall ocular structure. In the mouse eye for example, PAX6 overexpression leads to severe abnormalities such as microphthalmia and cataract formation<sup>53</sup> and

Glaser et al<sup>54</sup> have clearly shown a gene dosage effect of PAX6 in a human family in which different members were affected by PAX6 mutations with either full or only partial transcriptional activity.

Taken together, our data show that retinal ganglion cell death induces the expression of PAX6 in cells of the INL. This suggests that PAX6 might be involved in the maintenance of the cellular integrity after the loss of synaptic connectivity and/or in processes required for the remodeling of the retinal cytoarchitecture after ganglion cell loss. Further studies looking at PAX6 expression in other mouse model of glaucoma would be interesting to confirm our findings.

### ACKNOWLEDGMENTS

The authors thank Jürgen Götz for providing the transgenic mice and Lars Ittner, Heiko Wurdak, and Lukas Sommer for their fruitful discussions, continuous support, and careful reading of the manuscript.

### REFERENCES

- Cvekl A, Tamm ER. Anterior eye development and ocular mesenchyme: new insights from mouse models and human diseases. *Bioessays*. 2004;26:374–386.
- Gehring WJ, Ikeo K. Pax 6: mastering eye morphogenesis and eye evolution. *Trends Genet*. 1999;15:371–377.
- Kozmik Z, Daube M, Frei E, et al. Role of Pax genes in eye evolution: a cnidarian PaxB gene uniting Pax2 and Pax6 functions. *Dev Cell*. 2003;5:773–785.
- Quiring R, Walldorf U, Kloter U, et al. Homology of the eyeless gene of *Drosophila* to the Small eye gene in mice and Aniridia in humans. *Science*. 1994;265:785–789.
- Altmann CR, Chow RL, Lang RA, et al. Lens induction by Pax-6 in *Xenopus laevis*. *Dev Biol*. 1997;185:119–123.
- Baulmann DC, Ohlmann A, Flugel-Koch C, et al. Pax6 heterozygous eyes show defects in chamber angle differentiation that are associated with a wide spectrum of other anterior eye segment abnormalities. *Mech Dev*. 2002;118:3–17.
- Collinson JM, Quinn JC, Hill RE, et al. The roles of Pax6 in the cornea, retina, and olfactory epithelium of the developing mouse embryo. *Dev Biol*. 2003;255:303–312.
- Lovicu FJ, Steven P, Saika S, et al. Aberrant lens fiber differentiation in anterior subcapsular cataract formation: a process dependent on reduced levels of Pax6. *Invest Ophthalmol Vis Sci*. 2004;45:1946–1953.
- Singh S, Mishra R, Arango NA, et al. Iris hypoplasia in mice that lack the alternatively spliced Pax6(5a) isoform. *Proc Natl Acad Sci U S A*. 2002;99:6812–6815.
- Azuma N, Yamaguchi Y, Handa H, et al. Mutations of the PAX6 gene detected in patients with a variety of optic-nerve malformations. *Am J Hum Genet*. 2003;72:1565–1570.
- Chao LY, Mishra R, Strong LC, et al. Missense mutations in the DNA-binding region and termination codon in PAX6. *Hum Mutat*. 2003;21:138–145.
- Hanson IM, Fletcher JM, Jordan T, et al. Mutations at the PAX6 locus are found in heterogeneous anterior segment malformations including Peters' anomaly. *Nat Genet*. 1994;6:168–173.
- Jordan T, Hanson I, Zaletayev D, et al. The human PAX6 gene is mutated in two patients with aniridia. *Nat Genet*. 1992;1:328–332.
- Lauderdale JD, Wilensky JS, Oliver ER, et al. 3' deletions cause aniridia by preventing PAX6 gene expression. *Proc Natl Acad Sci U S A*. 2000;97:13755–13759.
- Lines MA, Kozlowski K, Walter MA. Molecular genetics of Axenfeld-Rieger malformations. *Hum Mol Genet*. 2002;11:1177–1184.
- Mirzayans F, Pearce WG, MacDonald IM, et al. Mutation of the PAX6 gene in patients with autosomal dominant keratitis. *Am J Hum Genet*. 1995;57:539–548.
- Neethirajan G, Hanson IM, Krishnadas SR, et al. A novel PAX6 gene mutation in an Indian aniridia patient. *Mol Vis*. 2003;9:205–209.
- Zumkeller W, Orth U, Gal A. Three novel PAX6 mutations in patients with aniridia. *Mol Pathol*. 2003;56:180–183.
- Behrens M, Langecker TG, Wilkens H, et al. Comparative analysis of Pax-6 sequence and expression in the eye development of the blind cave fish *Astyanax fasciatus* and its epigeal conspecific. *Mol Biol Evol*. 1997;14:299–308.
- Cvekl A, Piatigorsky J. Lens development and crystallin gene expression: many roles for Pax-6. *Bioessays*. 1996;18:621–630.
- Duncan MK, Xie L, David LL, et al. Ectopic Pax6 expression disturbs lens fiber cell differentiation. *Invest Ophthalmol Vis Sci*. 2004;45:3589–3598.
- De Melo J, Qiu X, Du G, et al. Dlx1, Dlx2, Pax6, Brn3b, and Chx10 homeobox gene expression defines the retinal ganglion and inner nuclear layers of the developing and adult mouse retina. *J Comp Neurol*. 2003;461:187–204.
- Stanescu D, Iseli HP, Schwerdtfeger K, et al. Continuous expression of the homeobox gene Pax6 in the ageing human retina. *Eye (Lond)*. 2007;21:90–93.
- Ittner LM, Schwerdtfeger K, Kunz TH, et al. Transgenic mice with ocular overexpression of an adrenomedullin receptor reflect human acute angle-closure glaucoma. *Clin Sci (Lond)*. 2008;114:49–58.
- Hafezi F, Abegg M, Grimm C, et al. Retinal degeneration in the rd mouse in the absence of c-fos. *Invest Ophthalmol Vis Sci*. 1998;39:2239–2244.
- Winkler BS, Giblin FJ. Glutathione oxidation in retina: effects on biochemical and electrical activities. *Exp Eye Res*. 1983;36:287–297.
- Xu PX, Zhang X, Heaney S, et al. Regulation of Pax6 expression is conserved between mice and flies. *Development*. 1999;126:383–395.
- Bhat SP, Rayner SA, Huang CM, et al. Quantitative estimation of RNA transcripts suggests persistence of Pax-6 expression in the postembryonic chick retina. *Dev Neurosci*. 1999;21:140–146.
- Jones SE, Jomary C, Grist J, et al. Expression of Pax-6 mRNA in the retinal degeneration (rd) mouse. *Biochem Biophys Res Commun*. 1998;252:236–240.
- Zhang W, Cveklova K, Oppermann B, et al. Quantitation of PAX6 and PAX6(5a) transcript levels in adult human lens, cornea, and monkey retina. *Mol Vis*. 2001;7:1–5.
- Quigley HA, Broman AT. The number of people with glaucoma worldwide in 2010 and 2020. *Br J Ophthalmol*. 2008;90:262–267.
- Gross RL, Ji J, Chang P, et al. A mouse model of elevated intraocular pressure: retina and optic nerve findings. *Trans Am Ophthalmol Soc*. 2003;101:163–169; discussion 169–171.
- Grozdanic SD, Betts DM, Sakaguchi DS, et al. Laser-induced mouse model of chronic ocular hypertension. *Invest Ophthalmol Vis Sci*. 2003;44:4337–4346.
- Fu CT, Sretavan D. Laser-induced ocular hypertension in albino CD-1 mice. *Invest Ophthalmol Vis Sci*. 2010;51:980–990.
- Wang X, Tay SS, Ng YK. An immunohistochemical study of neuronal and glial cell reactions in retinas of rats with experimental glaucoma. *Exp Brain Res*. 2000;132:476–484.
- landiev I, Biedermann B, Bringmann A, et al. Atypical gliosis in Muller cells of the slowly degenerating rds mutant mouse retina. *Exp Eye Res*. 2006;82:449–457.
- Yuan L, Neufeld AH. Activated microglia in the human glaucomatous optic nerve head. *J Neurosci Res*. 2001;64:523–532.
- Whiteley SJ, Klassen H, Coffey PJ, et al. Photoreceptor rescue after low-dose intravitreal IL-1beta injection in the RCS rat. *Exp Eye Res*. 2001;73:557–568.
- Grimm C, Wenzel A, Hafezi F, et al. Gene expression in the mouse retina: the effect of damaging light. *Mol Vis*. 2000;6:252–260.

40. Yorio T, Krishnamoorthy R, Prasanna G. Endothelin: is it a contributor to glaucoma pathophysiology? *J Glaucoma*. 2002;11:259–270.
41. Diem R, Taheri N, Dietz GP, et al. HIV-Tat-mediated Bcl-XL delivery protects retinal ganglion cells during experimental autoimmune optic neuritis. *Neurobiol Dis*. 2005;20:218–226.
42. Lin HL, Yang JS, Yang JH, et al. The role of Ca<sup>2+</sup> on the DADS-induced apoptosis in mouse-rat hybrid retina ganglion cells (N18). *Neurochem Res*. 2006;31:383–393.
43. Petrin D, Baker A, Coupland SG, et al. Structural and functional protection of photoreceptors from MNU-induced retinal degeneration by the X-linked inhibitor of apoptosis. *Invest Ophthalmol Vis Sci*. 2003;44:2757–2763.
44. Renwick J, Narang MA, Coupland SG, et al. XIAP-mediated neuroprotection in retinal ischemia. *Gene Ther*. 2006;13:339–347.
45. Schuettauf F, Rejdak R, Walski M, et al. Retinal neurodegeneration in the DBA/2J mouse—a model for ocular hypertension. *Acta Neuropathol*. 2004;107:352–358.
46. Libby RT, Anderson MG, Pang IH, et al. Inherited glaucoma in DBA/2J mice: pertinent disease features for studying the neurodegeneration. *Vis Neurosci*. 2005;22:637–648.
47. Schwartz M, Yoles E. Optic nerve degeneration and potential neuroprotection: implications for glaucoma. *Eur J Ophthalmol*. 1999;9(suppl 1):S9–11.
48. Sun Q, Ooi VE, Chan SO. N-methyl-D-aspartate-induced excitotoxicity in adult rat retina is antagonized by single systemic injection of MK-801. *Exp Brain Res*. 2001;138:37–45.
49. Vorwerk CK, Lipton SA, Zurakowski D, et al. Chronic low-dose glutamate is toxic to retinal ganglion cells. Toxicity blocked by memantine. *Invest Ophthalmol Vis Sci*. 1996;37:1618–1624.
50. Buchi ER. Cell death in rat retina after pressure-induced ischaemia-reperfusion insult: electron microscopic study. II. Outer nuclear layer. *Jpn J Ophthalmol*. 1992;36:62–68.
51. Marc RE, Jones BW, Watt CB, et al. Neural remodeling in retinal degeneration. *Prog Retin Eye Res*. 2003;22:607–655.
52. Ashery-Padan R, Gruss P. Pax6 lights-up the way for eye development. *Curr Opin Cell Biol*. 2001;13:706–714.
53. Schedl A, Ross A, Lee M, et al. Influence of PAX6 gene dosage on development: overexpression causes severe eye abnormalities. *Cell*. 1996;86:71–82.
54. Glaser T, Jepeal L, Edwards JG, et al. PAX6 gene dosage effect in a family with congenital cataracts, aniridia, anophthalmia and central nervous system defects. *Nat Genet*. 1994;7:463–471.